

AN INVESTIGATION ON THE INFLUENCE OF LOADING RATE ON THE FRACTURE TOUGHNESS OF UHMW-PE COMPOSITES

Michael May, Torsten R. Lässig and Stefan J. Hiermaier

Fraunhofer-Institute for High-Speed Dynamics, Ernst-Mach-Institut EMI,
Eckerstr. 4, 79104 Freiburg, Germany

Email: michael.may@emi.fraunhofer.de, Web Page: <http://www.emi.fraunhofer.de>

Keywords: Fracture toughness, Mechanical Testing, Computational modeling, Strain rate

Abstract

Ultra-high molecular weight polyethylene composites are frequently used in ballistic impact applications. For predictive modeling of impact scenarios it is important to consider potential effects of loading rate on the mechanical properties of the composite – especially the fracture toughness. In this article, the influence of loading rate on the mode I fracture toughness of Dyneema® HB26 is studied. It was found that the fracture toughness increases with increasing loading rate. A material model for cohesive interface elements is proposed which includes both, the rate dependency of the mode I fracture toughness and the rate dependency of the out-of-plane tensile strength. The model is implemented into ABAQUS/Explicit and verified against the experimental evidence.

1. Introduction

Over the last decade ballistic composites made from ultra-high molecular weight polyethylene (UHMW-PE) fibers have gained a lot of attention in personal armor and vehicle armor systems due to their extraordinary ballistic performance [1-3]. The response of ultra-high molecular weight polyethylene UHMW-PE composite panels subjected to ballistic impact loading is governed by two different failure mechanisms, namely shear plugging during the initial penetration followed by delamination and the formation of a bulge at backside of the panel [4]. The design process of armor systems incorporating UHMW-PE composites requires accurate estimations of the size of the bulge as this may affect passengers inside a vehicle or police or military personal equipped with personal armor. Numerical simulation can be a valuable tool in order to predicting the response of UHMW-PE under impact loading. Cohesive interface elements are a powerful approach for predicting the onset and propagation of delamination in composites subjected to out-of-plane loading [5]. This is due to the fact that damage initiation and subsequent propagation can be captured in a single coherent simulation [6]. Commonly this is achieved by combining a strength based damage initiation criterion with an energy based failure criterion. May [7] showed that rate effects must be captured by the constitutive law if cohesive interface elements are used for impact applications. This article therefore describes an experimental approach to assess the effect of loading rate on the mode I fracture toughness in UHMW-PE composites. Based on these experimental observations a novel material model is derived incorporating the rate-dependent interface strength as well as the rate-dependent fracture toughness. The model is implemented into the explicit FE code ABAQUS/Explicit and verified by modeling the characterization experiments.

2. Material under investigation

The material analyzed in this paper is Dyneema® HB26 which is a ballistic composite used in personal armor such as protective vests and helmets but also in vehicle armor. This material comprises of several sheets of UHMW-PE fibers, manufactured in a gel-spinning and hot drawing process, oriented in $[0/90]_n$ cross-ply stacks. The fibers are enclosed in polyurethane resin (17% resin weight fraction) and hot pressed for consolidation. One outstanding property of Dyneema® HB26 is a density of 0.9 kg/m^3 and consequently an excellent specific strength of the composite which is most important for ballistic applications.

3. Material properties

3.1. Mode I fracture toughness

The most critical parameter for describing the delamination response of composites is the mode I fracture toughness. Classically, this material parameter is measured using the standardized double cantilever beam (DCB) test [8]. The standard specimen used for this test is a slender with a Teflon insert on one end in order to induce a pre-crack. However, we found that the standard specimen geometry is not suitable for measuring the mode I fracture toughness of Dyneema® HB26 [9]. If the standard test procedure is followed, the arms of the DCB specimen break due to the relatively low in-plane stiffness of the material and the low out-of-plane strength. This phenomenon is also known from composites with extremely strong interfaces, for example in the case of through-thickness reinforced composites. Dransfield and co-workers [10-11] overcame this problem by bonding metallic tabs onto the DCB arms in order to increase the bending stiffness of the arms and therefore avoid breaking of the composite arms. When adopting this approach for Dyneema® HB26 we found that this solution also does not work. UHMW-PE composites are materials which do not bond very well resulting in debonding of the metallic tabs during delamination testing. Consequently, the only way forward in measuring the fracture toughness of Dyneema® HB26 was the use of very thick specimens as shown in Fig. 1.

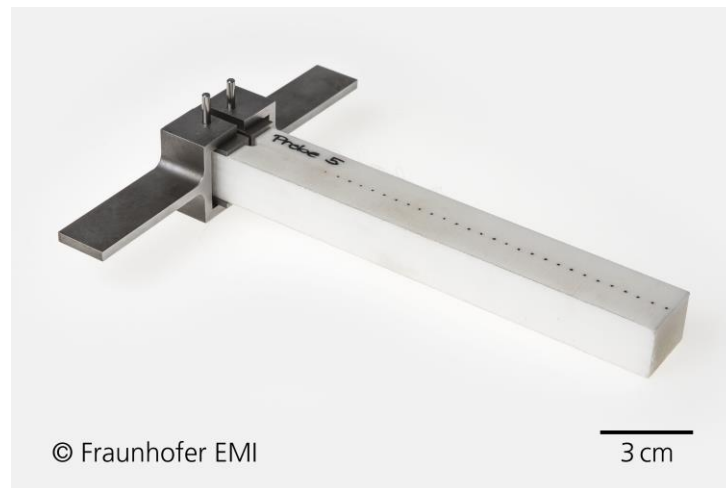


Figure 1. Thick DCB specimen used for determining the mode I fracture toughness.

A Dyneema® panel of dimensions 400 mm x 400 mm x 26 mm was hot-pressed using a pressure of 165 bar. Teflon inserts were placed on two opposite edges of the panel in order to introduce pre-cracks in the mid-plane of the panel. The specimens were then waterjet-cut from the panel as we found that machining with milling machines or blades did not result in adequate quality.

Measurements of the mode I fracture toughness of composites under high rates of loading may be affected by inertia effects which result in asymmetric, and therefore mixed-mode loading conditions [12-13]. In a recent review on the measurement of mode I fracture toughness of composites under high rates of loading, May therefore recommended the use of a wedge pushed between the specimen arms by a servo-hydraulic machine in order to enforce symmetric opening of the DCB specimen [14]. In the work reported here, the DCB specimens were tested in the classical configuration (without a wedge) at constant crosshead displacement rates of 1 mm/s, 10 mm/s and 100 mm/s. This was feasible as these three test velocities are below the critical velocity where inertia effects have to be accounted for. U-shaped metallic caps were placed around the load introduction points in order to reinforce the pin-loaded region. Loads were recorded using a Hammer load cell of capacity 1000 N. Each test was recorded with a high-speed camera, type Photron FASTCAM SA5 and a magnifying lense. The images recorded during the tests were later used to determine the crack length. During the tests it was observed that several cracks appeared in neighboring plies to the dominant crack in the mid-surface, especially for the quasi-static and medium rate load case. This was due to the fact that the out-of-plane strength of Dyneema® HB26 is extremely low as shown in [15]. As a consequence, evaluation methods such as the modified beam theory are not valid anymore. The fracture toughness was therefore evaluated by using the area method.

$$G_{Ic} = \frac{W_{total} - W_{elastic}}{B \cdot a_{eff}} \quad (1)$$

Where W_{total} is the total area underneath the experimental force-displacement curve, $W_{elastic}$ is the elastic energy stored in the DCB, B is the specimen width, and a_{eff} is the effective crack length defined as the sum of the length of all cracks through the thickness of the beam. The procedure is detailed in [9].

Figure 2 shows the calculated fracture toughness as a function of loading velocity. No influence of loading rate is seen for velocities up to 10 mm/s ($G_c=460 \text{ J/m}^2$, COV 13,0%). A strong increase of fracture toughness is observed for loading velocity of 100 mm/s ($G_c=785 \text{ J/m}^2$, COV 16,6%).

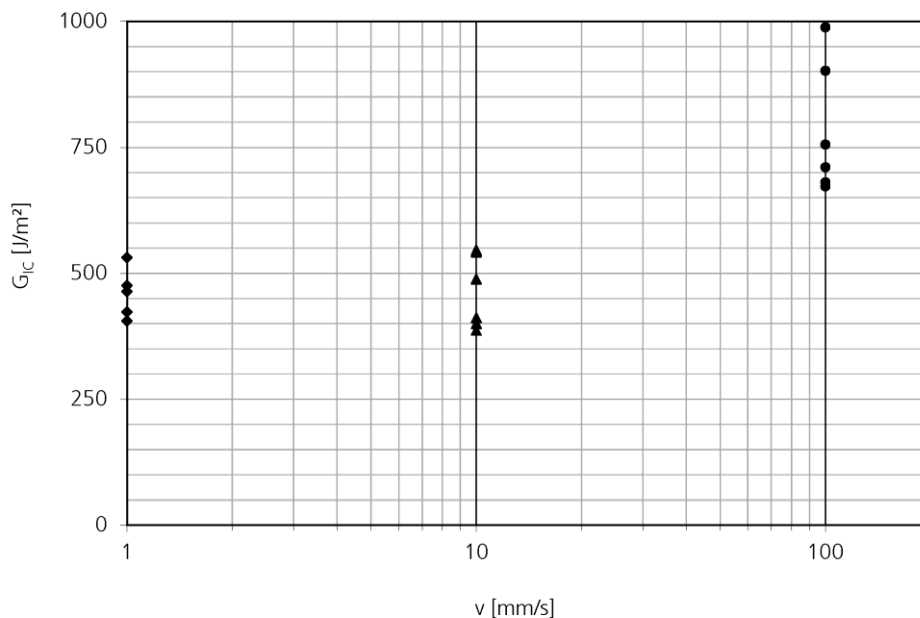


Figure 2. Measured fracture toughness as a function of loading velocity.

3.2. Out-of-plane tensile strength

The second material parameter of importance for describing the delamination response of composites using cohesive zone models is the mode I strength of the material. The delamination response of composite materials is dominated by the properties of the resin [16-17]. It is therefore postulated that data on pure polyurethane can be used for describing the through-thickness strength of Dyneema® HB26 composite. Sarva et al. [18] have characterized polyurethane for a wide range of strain rates (from 0.002 s⁻¹ to 7800 s⁻¹). This data is displayed using diamonds in Fig. 3.

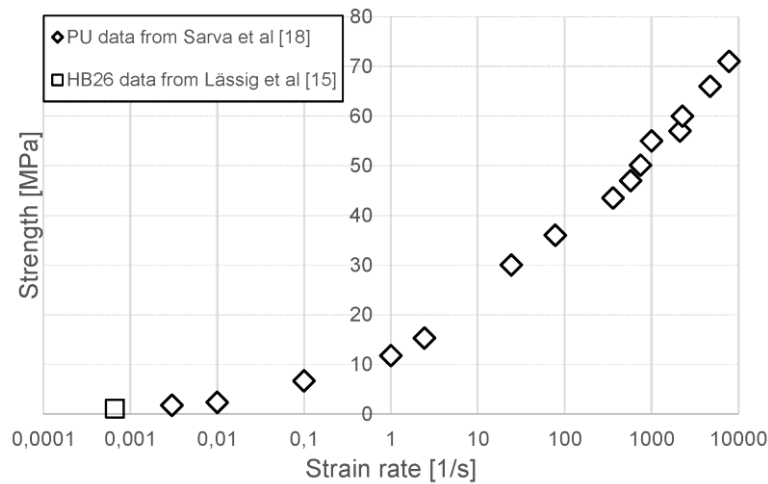


Figure 3. Evolution of out-of-plane tensile strength as a function of strain rate.

Quasi-static data measured on Dyneema® HB26, reported by Lässig et al. [15] is added by a square. It becomes obvious that the data provided by Lässig et al. [15] on composite matches perfectly well with the PU data taken from Sarva et al. [18] indicating the validity of the previous assumption. The evolution of out-of-plane strength with strain rate can be described by a quadratic function of the strain rate if plotted on a semi-logarithmic scale.

4. Modeling approach

4.1. General formulation

The basic cohesive zone modeling approach adopted in this article follows the suggestions by Jiang et al. [18]. In the following the full mixed-mode formulation is briefly described although only mode I load cases are treated within this article.

Damage initiation is described by a quadratic stress based criterion

$$\sqrt{\left(\frac{\max(\sigma_I, 0)}{\sigma_I^{\max}}\right)^2 + \left(\frac{\sigma_{II}}{\sigma_{II}^{\max}}\right)^2} = 1, \quad (2)$$

where σ_I , σ_{II} are the current stresses in thickness and shear direction and σ_I^{\max} , σ_{II}^{\max} are the maximum interface stresses in thickness and shear direction, respectively. As shown in [19], the displacement at damage initiation δ_m^e can be calculated using equation (3)

$$\delta_m^e = 1 / \sqrt{\left(E_I \cos I / \sigma_I^{\max}\right)^2 + \left(E_{II} \cos II / \sigma_{II}^{\max}\right)^2} = 1 \quad (3)$$

where E_I , E_{II} are the mode I and mode II interface stiffness and $\cos I$, $\cos II$ are the direction cosini defined in [19].

The interface behaves linear-elastic before the damage initiation criterion is met. If the interface is loaded beyond δ_m^e , the strength is degraded linearly until complete failure of the interface. A quadratic, energy-based failure criterion is adopted to describe complete interface failure.

$$\left(\frac{G_I}{G_{Ic}}\right)^2 + \left(\frac{G_{II}}{G_{IIc}}\right)^2 = 1, \quad (4)$$

where G_I , G_{II} are the mode I and mode II energies stored in the cohesive interface element and G_{Ic} , G_{IIc} are the mode I and mode II fracture toughness, respectively. Following [19], the displacement at complete failure δ_m^f can be calculated using equation (5)

$$\delta_m^f = \frac{1}{\sqrt{\left(\frac{\sigma_I^Y \cos I}{2 \cdot G_{Ic}}\right)^2 + \left(\frac{\sigma_{II}^Y \cos II}{2 \cdot G_{IIc}}\right)^2}}, \quad (5)$$

Where σ_I^Y , σ_{II}^Y are the mode I and mode II stresses at damage initiation as defined in [19]. The mixed-mode damage parameter is 0 at the beginning of the simulation and 1 at complete failure of the interface element. A linear evolution of damage parameter with increasing traction δ_m is ensured by defining the damage parameter as follows

$$D(\delta_m) = \frac{\delta_m - \delta_m^e}{\delta_m^f - \delta_m^e}, \quad (6)$$

4.2. Rate-dependent material properties

Following the suggestions by May and co-workers [20-21] the strain rate dependent mode I strength is described by a piece-wise function. For strain rates exceeding a certain threshold value, the strain rate dependent mode I strength can be described by a quadratic function on a semi-logarithmic scale. This function is derived from the graph shown in Fig. 3 which was derived from PU data taken from [18] and the additional Dyneema® HB26 data point taken from [15]. The strength below a threshold, defining quasi-static conditions, is assumed to be constant.

$$\sigma_I^{\max}(\dot{\epsilon}_I) = \begin{cases} C_1 \cdot (\log \dot{\epsilon}_{ref})^2 + C_2 \cdot \log \dot{\epsilon}_{ref} + C_3 & \text{for } \dot{\epsilon}_I \leq \dot{\epsilon}_{ref} \\ C_1 \cdot (\log \dot{\epsilon}_I)^2 + C_2 \cdot \log \dot{\epsilon}_I + C_3 & \text{for } \dot{\epsilon}_I > \dot{\epsilon}_{ref} \end{cases} \quad (7)$$

where C_1, C_2, C_3 are constants describing a parabolic function, $\dot{\epsilon}_I$ is strain rate in through-thickness direction of the cohesive element and $\dot{\epsilon}_{ref}$ is the reference strain rate defining quasi-static loading conditions. Following a similar logic, the rate dependent evolution of the mode I fracture toughness is described by a piece-wise function. For loading rates below a threshold value (in this case 10 mm/s), the fracture toughness is assumed to be constant. For loading rates exceeding the threshold, the fracture toughness can be described as a function of loading velocity.

$$G_{Ic}(v) = \begin{cases} G_{Ic} & \text{for } v \leq v_{ref} \\ G_{Ic} + C_4 \cdot \log\left(\frac{v}{v_{ref}}\right) & \text{for } v > v_{ref} \end{cases} \quad (8)$$

5. FINITE ELEMENT SIMULATION

The model described in the previous section was implemented into the explicit FE code ABAQUS/Explicit by means of a user-defined material model (VUMAT). The model was verified by computing the response of the thick DCB specimens used for calibrating the model. The arms of the beam were modeled using fully integrated solid elements, type C3D8 in order to avoid hourglassing. A single potential crack path was introduced in the center of the thick DCB specimen using cohesive interface elements, type COH3D8, thickness 0.1 mm. This is a simplification compared with the experimental results, where several cracks formed during loading. However, as the analysis of the experiments was based on a total effective crack length, this simplification is thought to be representative. An estimation of the cohesive zone length following Harper and Hallett [22] indicated extremely long cohesive zones for Dyneema® HB26. Therefore, a relatively coarse mesh of element length 2 mm could be used which would still show convergence. One node was created in the geometric center of each hole (top and bottom) drilled through the metallic part and the Dyneema® specimen. These nodes were connected to the surrounding nodes via MPC. A constant velocity was applied to the upper node as shown in Fig. 4. The lower arm was pinned (translational DOF fixed, rotational DOF free) at the node. No mass scaling was used for the high-rate load case. Selective mass scaling was used for quasi-static and medium rate loading in order to speed up the simulation. Inertia was negligible compared to the total energy in the model. For comparison, the simulations were performed with the fully rate dependent model and for specific pre-defined maximum strengths of the interface.

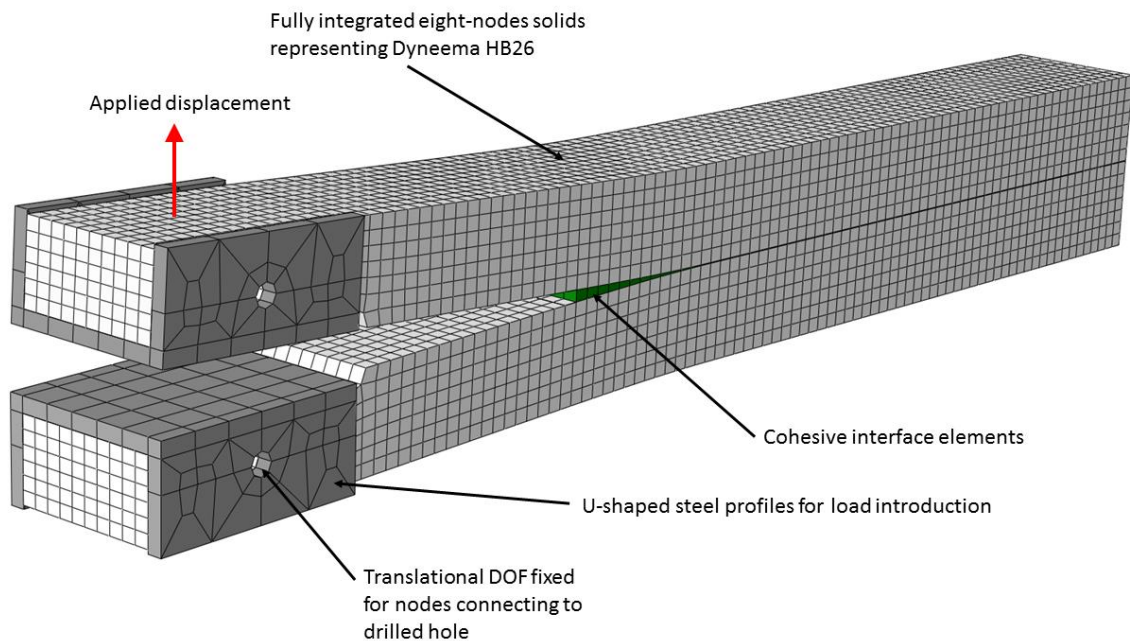


Figure 4. Setup of finite element model.

Figure 5 compares the predicted force-displacement curve (dashed red line) to the experimental results (solid grey lines) for the high-rate load case. In general the shape of the force displacement curve is captured well. However, the predicted initial stiffness is too low. A parametric study with pre-defined maximum interface stresses showed that the maximum interface stress has some influence on the initial stiffness of the simulation. This is due to the fact that the relatively low maximum interface stress results in a rather large cohesive zone length and therefore in softening of the whole structure.

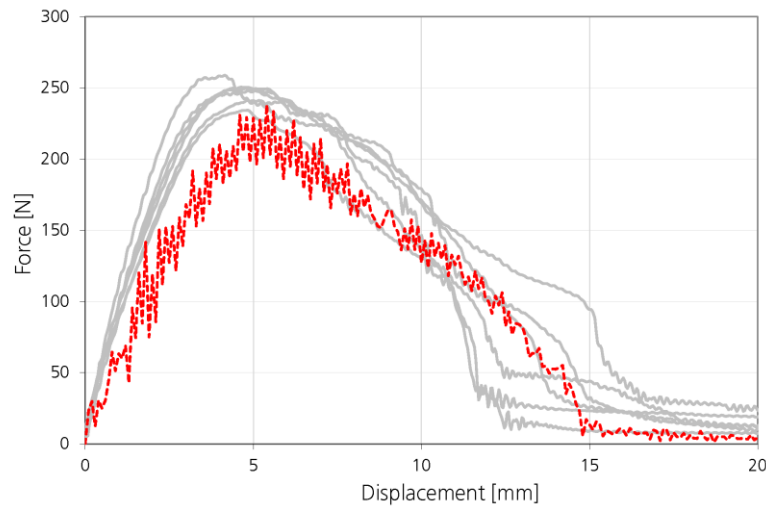


Figure 5. Comparison of FE simulation and experiment.

For lower loading velocities the force-displacement curve was significantly underpredicted indicating that the simplifications suggested for evaluating the fracture toughness may not be valid.

6. Conclusions and Outlook

The mode I fracture toughness of Dyneema® HB26 was measured experimentally for loading velocities ranging from 1 mm/s to 100 mm/s. The fracture toughness was found to increase with increasing loading velocity for velocities greater than 10 mm/s. A material model is proposed allowing capturing of these rate effects. The model is implemented in Abaqus/Explicit and verified against the experimental data. Future work will focus on translation of loading velocity into local strain rate in order to allow the model to be used to predict delamination in complex impact scenarios. Additionally, the experimental evaluation of fracture toughness has to be revisited for the cases with several cracks running at the same time.

Acknowledgments

The authors would like to thank Dr. Ulrich Heisserer and Dr. Harm van der Werff from DSM for manufacturing the Dyneema® HB26 panels. Additionally the authors thank Mr. Florian Schneider for the help with the experimental work and Mr. René Groß for support with image processing.

References

- [1] U. Heisserer and H. van der Werff. The relation between Dyneema fiber properties and ballistic protection performance of ist fiber composites. *Proceedings of the 15th International Conference on Deformation, Yield and Fracture of Polymers, Kerkrade, The Netherlands, 2012.*
- [2] L. Vargas-Gonzalez, S. Walsh and B. Scott. Balancing the back-face deformation in helmets: the role of alternative resins, fibers, and fiber architectures in mass efficient head protection. *Proceedings of the 26th International Symposium on Ballistics, Miami, USA, 2011.*
- [3] B. Lee J. Song and J Ward. Failure of Spectra polyethylene fiber-reinforced composites under ballistic impact loading. *Journal of Composite Materials, 28:1202-1226, 1994.*

- [4] L. Nguyen, S. Ryan, S. Cimoperu, A. Mouritz and A. Orifici. The effect of target thickness on the ballistic performance of ultrahigh molecular weight polyethylene composites. *International Journal of Impact Engineering*, 75:174-183, 2015.
- [5] M. Wisnom. Modelling discrete failures in composites with interface elements. *Composites Part A*, 41(7):795-805, 2010.
- [6] M. May and S. Hallett. A combined model for initiation and propagation of damage under fatigue loading for cohesive interface elements. *Composites Part A*, 41(12):1787-1796, 2010.
- [7] M. May. Numerical evaluation of cohesive zone models for modeling impact induced delamination in composite materials. *Composite Structures*, 133:16-21, 2015.
- [8] ASTM D-5528-01: Standard Test Method for Mode I Interlaminar Fracture Toughness of Unidirectional Fibre-Reinforced Polymer Matrix Composites, 2001.
- [9] T. Lässig, F. Nolte, W. Riedel, M. May. An assessment of experimental techniques for measuring Mode I fracture toughness of UHMW-PE composites. *Proceedings of the 17th European Conference on Composite Materials ECCM17*, Munich, 2016.
- [10] L. Jain, K. Dransfield and Y-W. Mai. Effect of Reinforcing Tabs on the Mode I Delamination Toughness of Stitched CFRPs. *Journal of Composite Materials*, 32:2016-2041, 1998.
- [11] K. Dransfield, L. Jain and Y-W. Mai. On the effects of stitching in CFRPs - I. Mode I delamination toughness. *Composites Science and Technology* 58(6):815-827, 1998
- [12] G. Hug, P. Thévenet, J. Fitoussi and D. Baptiste. Effect of loading rate on mode I interlaminar fracture toughness of laminated composites. *Engineering Fracture Mechanics*, 73:2456-2462, 2006.
- [13] M. Colin de Verdiere, A. Skordos, M. May and A. Walton. Influence of loading rate on the delamination response of untufted and tufted carbon epoxy non crimp fabric composites: Mode I. *Engineering Fracture Mechanics*, 96:11-25, 2012.
- [14] M. May. Measuring the rate-dependent mode I fracture toughness of composites – A review. *Composites: Part A*, 81:1-12, 2016
- [15] T. Lässig, L. Nguyen, M. May, W. Riedel, U. Heisserer, H. van der Werff and S. Hiermaier. A non-linear orthotropic hydrocode model for ultra-high molecular weight polyethylene in impact simulations. *International Journal of Impact Engineering*, 75:110-122, 2015.
- [16] D. Krause. A physically based micromechanical approach to model damage initiation and evolution of fiber reinforced polymers under fatigue loading conditions. *Composites Part B*, 87:176-195, 2016.
- [17] M. May and S. Hallett. Damage initiation in polymer matrix composites under high-cycle fatigue loading – A question of definition or a material property? *International Journal of Fatigue*, 87:59-62, 2016.
- [18] S. Sarva, S. Deschanel, M. Boyce and W. Chen. Stress-strain behavior of a polyurea and a polyurethane from low to high strain rates. *Polymer*, 48:2208-2213, 2007.
- [19] W. Jiang, S. Hallett, B. Green and M. Wisnom. A concise interface constitutive law for analysis of delamination and splitting in composite materials and its application to scaled notched tensile specimens. *International Journal for Numerical Methods in Engineering*, 69(9):1982-1995, 2007.
- [20] M. May, H. Voß and S. Hiermaier. Predictive modeling of damage and failure in adhesively bonded metallic joints using cohesive interface elements. *International Journal of Adhesion and Adhesives*, 49:7-17, 2014.
- [21] M. May, O. Hesebeck, S. Marzi, W. Böhme, J. Lienhard, S. Kilchert, M. Brede and S. Hiermaier. Rate dependent behavior of crash-optimized adhesives – Experimental characterization, model development, and simulation. *Engineering Fracture Mechanics*, 133:112-137, 2015.
- [22] P. Harper and S. Hallett. Cohesive zone length in numerical simulations of composite delamination. *Engineering Fracture Mechanics*, 75(16):4774-4792, 2008.